Permeability estimates of porous media from Induced Polarization data: preliminary results

Marianna Tagnin*[1], Andréa T. Ustra[1], Carlos A. Mendonça[1], Carlos A. M. Chaves[1], José L. Albuquerque Filho[2], Humberto R. da Rocha[1], [1] Instituto de Astronomia, Geofísica e Ciências Atmosféricas - USP, [2] Instituto de Pesquisas Tecnológicas do Estado de São Paulo - IPT

Abstract

Hydrogeological research is fundamental to guarantee water and food security, being one of the main branches of action at the Center for Water and Food Security in Critical Zones (Centro para Segurança Hídrica e Alimentar em Zonas Críticas - CSHAZC). Direct investigation methods (e.g., drilling and monitoring wells) are largely employed in Hydrogeology, providing precise and valuable information on the subsurface and water quality, although in point-scale and subject technically to rather shallow investigations. Geophysical methods investigate the subsurface indirectly through the spatial distribution of its physical properties, allowing for a larger-scale investigation. DC Resistivity and Induced Polarization (IP) are sensitive to hydraulic properties of the medium, and recent studies established relationships between IP and permeability, a key hydrogeological parameter. This work aims to contribute with CSHAZC estimating permeability for the Ribeirão das Posses sub-basin in Extrema, Minas Gerais, Brazil, obtaining its spatial variability. Preliminary results are presented for synthetic datasets based on the study area's soil composition.

Introduction

Water security, closely related to energy and food security (FAO, 2014), is achieved when there's sufficient quality water available for human needs, economical activities, and environmental preservation, while still considering and managing risks associated with extreme events like floods and droughts (ANA, 2019). The guarantee of water security relies on efficient public policies, which set the course of actions to achieve it and regulates water use and exploration, and on scientific data to deepen the understanding we have on these resources while also guiding public policies.

The Center for Water and Food Security in Critical Zones (Centro para Segurança Hídrica e Alimentar em Zonas Críticas - CSHAZC) aims to contribute with scientific data and solutions for water and food security in the state of São Paulo, Brazil. The Critical Zone (CZ), defined as the surface region between canopy and groundwater base supporting life on Earth (Brantley et al., 2007), allows for a transdisciplinary approach to investigate the medium and the ongoing natural and anthropic processes affecting it, with methodologies from the most diverse areas of science (Brantley et al., 2017), contributing with a more detailed understanding of the environment.

Hydrogeological studies usually employ direct investigation methods, such as drilling and recovering of core samples and installation of monitoring wells, providing valuable information on groundwater quality and medium properties, e.g., permeability (Binley et al., 2015). However, the sampling occurs in point scale, limited technically to the most superficial portion of the subsurface, and the techniques are invasive and costly.

On the other hand, geophysical methods make it possible to investigate the subsurface indirectly by providing information on the spatial variability of its physical properties. The techniques enable the acquisition of large data sets in extensive areas, even those with difficult access, in a non-invasive way, potentially reducing acquisition time and operation costs, and allowing for test repeatability and monitoring of the study area (Parsekian et al., 2015).

Geoelectrical methods like DC Resistivity and Induced Polarization (IP) are frequently employed in hydrogeological studies because of their sensitivity to hydraulic properties of the medium (Slater et al., 2014). Specifically, IP relates to superficial grain effects, being sensitive to textural and grain properties like tortuosity (Blondel et al., 2014). Since permeability is closely related to grain properties, there has been a lot of effort in the indirect estimation of this property, aiming for the determination of its spatial distribution (Weller & Slater, 2019).

Previous studies established relations between IP measurements and permeability empirically and through mechanistic models (e.g., Revil & Florsch, 2010; Robinson et al., 2018; Weller & Slater, 2019). Empirical models rely on large datasets and unfortunately are valid only for similar geological conditions. Through mechanistic models it is possible to relate electrical information to grain size (e.g., Leroy et al., 2008), therefore, to permeability.

We aim to contribute with hydrogeological models for the CSHAZC's test area, Ribeirão das Posses sub-basin in Extrema, Minas Gerais, Brazil. Our proposal is to characterize and monitor groundwater with DC Resistivity and IP, and specifically through IP measurements estimate

permeability for the study area, obtaining its spatial distribution.

The objective of this work is to test one permeability model directly related to the IP mechanistic model's key parameters for a synthetic dataset based on the study area's lithology.

Method

The study area is the Ribeirão das Posses hydrographic sub-basin, in the city of Extrema, Minas Gerais, Brazil (Figure 1). It is part of the Rio Jaguari system, which is a tributary of the Cantareira system, an important water supply for the metropolitan area of São Paulo.

Previous studies have been conducted in the area and it is currently being monitored to deepen the understanding of the hydrological regime in a catchment basin and provide scientific data to guide public policies in a reforestation area.

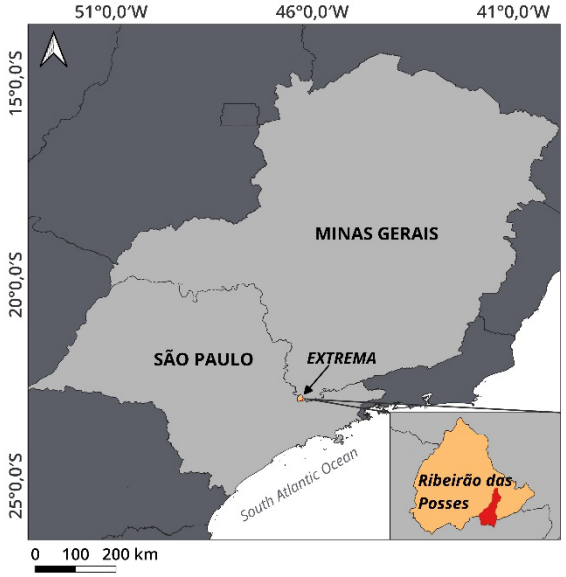

***Figure 1** - Study area location, highlighting the Ribeirão das Posses sub-basin in red.*

Kowalski (2022) identified through DC Resistivity acquisitions two main geoelectrical units associated with saprolite covering bedrock of granitic-gneiss composition. According to Silva (2019), the main types of soils found in the Ribeirão das Posses sub-basin are Argissolo Vermelho and Argissolo Vermelho-Amarelo, with varying proportions of sand and clay.

The Induced Polarization (IP) method

The IP method measures the IP effect, characterized by the lagged response of the medium to the passage of electric current, which causes its polarization due to the storage of charges, estimating the time necessary for the material to return to its natural state, not electrically disturbed.

Acquisitions can be performed in the time domain, obtaining chargeability (m) and normalized chargeability (m_n), given by equations (1) and (2), respectively. Chargeability measures the magnitude of the IP effect, and normalized chargeability is an estimation of the material's polarizability.

$$m = \frac{1}{\Delta V_c}\int_{t_1}^{t_2} v(t)dt \quad (1)$$

$$m_n = \frac{m}{\rho} \quad (2)$$

Acquisitions can also be performed in the frequency domain, obtaining complex conductivity (σ^*), or its inverse, complex resistivity (ρ^*), and the phase (φ), given by equations (3) and (4), respectively, with angular frequency $\omega = 2\pi f$ and period $T = 1/f$.

$$\sigma^*(\omega) = \sigma'(\omega) + i\sigma''(\omega) = |\sigma|e^{i\omega\varphi} \quad (3)$$

$$\varphi = arctan\left(\frac{\sigma''}{\sigma'}\right) \quad (4)$$

There are two main polarization processes that can be distinguished in the usual range of operations (1 mHz to 1 kHz): the polarization of the Electrical Double Layer (EDL) prevails until approximately 100 Hz, which is directly related to the grains and particle size distributions; at higher frequencies (10 MHz) the Maxwell-Wagner dominates the signal (Revil & Florsch, 2010). Our focus is on the EDL polarization.

The real σ' (or in phase) component of the complex conductivity corresponds to ohmic conduction and dielectric losses. The imaginary σ'' (or in quadrature) component corresponds to capacitive conductivity, especially at low frequencies (f < 100 Hz), corresponding to the IP effect. In this range, the imaginary component is sensitive to textural grain parameters, e.g. tortuosity, and variations in the grain-fluid interface (Blondel et al., 2014). Also, in this range and domain, it is possible to mathematically derive relationships between IP data and petrophysical parameters like permeability.

At field scale, IP data is usually obtained in the time domain, while frequency domain data is more common in the laboratory scale (Martin et al., 2021). There are already established relationships between both domains: phase and chargeability can be considered analogous, normalized chargeability is directly proportional to imaginary conductivity (Ustra, 2017). Blanchy et al. (2020) reports that, at frequencies lower than 10 Hz, chargeability and phase are linearly related and complex impedance can be obtained from time domain IP data.

IP data fitting

IP data in the frequency domain can be challenging to interpret because the signal results from the superposition of polarization processes, being frequent to fit measured data with empirical or phenomenological models. Mechanistic models define each polarization process as one characteristic relaxation time (given in seconds) (Ustra et al., 2016), which represents the time it takes for the material to return to its natural unpolarized state. This

characteristic relaxation time (τ_0) relates to the grain diameter (d_0) by:

$$\tau_0 = \frac{d_0^2}{8D_i} \quad (5)$$

with D_i the diffusion coefficient of an *i* ion species (Revil & Florsch, 2010). The relaxation phenomena can be described by a Debye distribution, a particular case of the Cole-Cole model that considers only one relaxation time. The superposition of polarization processes will be given by the superposition of Debye distributions, resulting in the phenomenological model known as Debye decomposition (DD) (Ustra et al., 2016).

Data inversion techniques are applied to fit these models to IP measured data. The regularization method is advised in electrical imaging problems to stabilize the solutions (Falzone et al., 2018), especially in DD approaches (Weigand & Kemna, 2016). We follow the procedures implemented by Ustra et al. (2016), whose formulation directly relates the inverted parameters to the mechanistic model's parameters, allowing for the determination of physical properties of the media.

The complex conductivity is given by:

$$\sigma^*(\omega) = \sigma^u + (\sigma_s^0 - \sigma_s^\infty)\int_0^\infty g(\tau)\left(\frac{1}{1+i\omega\tau}\right)d\tau \quad (6)$$

where σ^u is the experimental high-frequency, equivalent to $\sigma_{DC} + \sigma_s^\infty$, being σ_{DC} the DC conductivity, σ_s^0 and σ_s^∞ are the low ($\omega \to 0$) and high-frequency ($\omega \to \infty$) surface conductivities respectively, and $g(\tau)$ represents the distribution of relaxation times, normalized to preserve unit length:

$$\int_0^\infty g(\tau)d\tau = 1 \quad (7)$$

The procedure involves discretization of $g(\tau)$ for a finite pre-established set of M relaxation times using Dirac δ-distributions:

$$g(\tau) = \sum_{k=1}^{M} g_k \delta(\tau - \tau_0)\Delta\tau_k \quad (8)$$

Defining $p_k = g_k\Delta\tau_k$, preserving unit-length $\left(\sum_{k=1}^{M} p_k = 1\right)$, and $\Delta\sigma = \sigma_s^0 - \sigma_s^\infty$, equation (6) can be rewritten as:

$$\sigma^*(\omega) = \sigma^u + \Delta\sigma\sum_{k=1}^{M} p_k\left(\frac{1}{1+i\omega\tau}\right) \quad (9)$$

The inverted parameters σ^u, $\Delta\sigma$ and p_k can be easily related to mechanistic models' parameters. For instance, $\Delta\sigma \equiv m_n$, and the distribution of relaxation times p_k gives the characteristic relaxation times τ_k associated with each polarization process, related to grain parameters as shown in equation (5).

The characteristic relaxation times are related to a relaxation frequency (f_0) by $\tau_0 = 1/2\pi f_0$ and can be observed in a phase plot as a bell-shaped peak. Mathematically, these peaks can be understood as local maximum, meaning the derivative at this point (named critical point) is zero:

$$\left(\varphi(\omega = f_0)\right)' = 0 \quad (10)$$

More subtle disturbances in the IP spectrum can happen, not forming the expected bell-shape, but still affecting the variation rate of the phase curve, which can be evaluated step-wisely, helping distinguish weaker or overlapped polarization processes.

IP and permeability

Permeability (k) is a hydrological parameter intrinsically related to the composition and geometric disposition of material in a granular media and can be formulated as:

$$k = \frac{\Lambda^2}{8F} \quad (11)$$

where F is the formation factor derived from Archie's law (Archie, 1942) and Λ is a hydraulic length scale (Robinson et al., 2018). Revil et al. (2012) related τ_0 to Λ, which yields:

$$\tau_0 = \frac{\Lambda^2}{2D^+} \quad (12)$$

and substituting equation (12) on (11):

$$k_t = \frac{\tau_0 D^+}{4F} \quad (13)$$

with D^+ being the diffusion coefficient of the counterions, assuming values of 1,3x10^{-9} m^2/s for clean sands (Revil et al., 2012) and 3,8x10^{-12} m^2/s for clayey material (Revil, 2013).

Results and Discussion

Considering soil information from the study area, the synthetic dataset consisted of two main lithologies: a fine sand with grain diameter d=0,063x10^{-3}, and clay with grain diameter d=2x10^{-6}. Fine sand was chosen to test if the peaks from two grains of different lithologies and small diameters were distinguishable. Data was modeled after mechanistic IP models for particle size distributions based on the works of Leroy et al. (2008), Leroy and Revil (2009) and Revil & Florsch (2010). The water conductivity was 100x10^{-3} mS/m, porosity of 40% and cementation exponent 1,5. A random gaussian noise of median zero and standard deviation 0,5x10^{-10} was added.

The inversion procedure follows Ustra et al. (2016). Figure 2a-2c shows the phase plot for fine sand (2a), clay (2b) and an equal parts mixed sample of fine sand and clay (2c). The derivative is shown in a dashed gray line.

The derivative approach allowed for determination of the characteristic relaxation times. However, the procedure showed up to be sensitive to subtle changes in the variation rate of the phase curve possibly due to noise, consequently returning artificial relaxation times not related to the sample that were manually filtered. This emphasizes the importance of having direct information beforehand, such as granulometry, to constrain the model.

For fine sand, τ_0 was the same for both situations (fine-sand only and equal parts fine sand and clay) and matched

what was expected from the synthetic data. On the other hand, τ_0 for clay presented different values for it, though in the same magnitude order. On a clay-only sample, τ_0 differed slightly from what was expected, while on the mixed sample the correct value was retrieved. Clays are the smallest of lithologies and polarize at higher frequencies, which can lead to more noisy data, especially at the borders, affecting the relaxation frequency.

Table 1 presents τ_0 and respectives d_0 for each identified peak, and estimation of permeability according to equation (13) for the three samples, evaluating two possible values for the coefficient D^+, which present different magnitude orders.

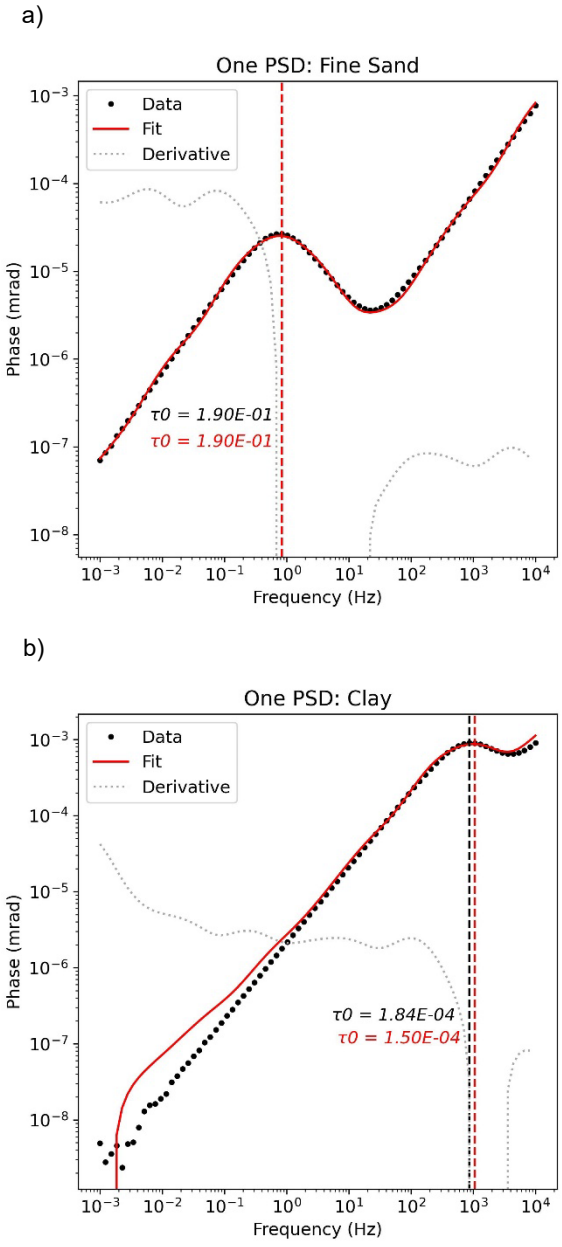

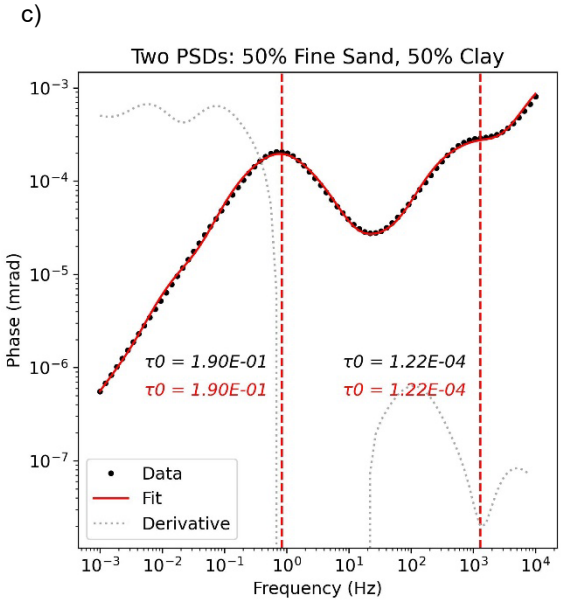

Figure 2 *- Frequency (Hz) vs. Phase (mrad) plot for a) fine sand sample, b) clay sample, and c) mixed sample (50% fine sand and 50% clay). The black dots are the synthetic data, the red continuous line is the calculated data from the inversion, and the dotted gray line is the derivative. Also shown are τ_0 from synthetic data (black) and from the inversion (red).*

Table 1 *- τ_0, d_0 and permeability k for the three samples. Permeability was estimated using two different values of D^+.*

Parameters	1 PSD: fine sand	1 PSD: clay	2 PSD: 50% fine sand, 50% clay
τ_0 [s]	$1{,}90\times10^{-1}$	$1{,}50\times10^{-4}$	$1{,}90\times10^{-1}$
			$1{,}22\times10^{-4}$
d_0 [m²]	$6{,}10\times10^{-5}$	$1{,}71\times10^{-6}$	$6{,}10\times10^{-5}$
			$1{,}55\times10^{-6}$
k [cm²]*	$1{,}56\times10^{-7}$	$1{,}23\times10^{-10}$	$7{,}82\times10^{-8}$
k [cm²]**	$4{,}57\times10^{-10}$	$3{,}60\times10^{-13}$	$2{,}28\times10^{-10}$

** D^+=1,3x10^{-9} m²/s for clean sands (Revil et al., 2012)*

*** D^+=3,8x10^{-12} m²/s for clayey material (Revil, 2013).*

Comparing to literature information (Feitosa et al., 2008), both estimates for permeability result in viable values and materials, although using D^+ of 3,8x10^{-12} m²/s for clayey material yields values that indicate the presence of clays. Since soil at Ribeirão das Posses sub-basin has clay in its composition, permeability estimates using D^+ for clayey material seems more adequate.

It's still necessary to evaluate this procedure in samples from the study area, retrieving granulometry information and checking if the values for D^+ from Revil et al. (2012) and Revil (2013), which were obtained for specific datasets, are adequate for the area's lithology.

Conclusions

The IP method can contribute with important information on hydrogeological properties indirectly, providing their spatial variability. Although the mathematical formulation relating IP and those parameters like permeability is done in the frequency domain, the relationship between both domains can potentially extend them to field-scale acquisitions, largely done in the time-domain.

This work explored IP mechanistic models and its petrophysical relationships, specifically with permeability, one key parameter in hydrogeological research. Three synthetic datasets were tested: one sample of fine sand, one sample of clay, and one sample of an equal parts mixture of fine sand and clay. The results, obtained through data inversion procedures using a Debye Decomposition phenomenological model, were satisfactory. The permeability estimates using a diffusion coefficient for clayey material were more realistic considering the range of materials encountered at Ribeirão das Posses sub-basin, whose soil composition includes sands and clays.

Acknowledgments

The authors acknowledge the Coordenação de Aperfeiçoamento de Pessoal de Nível Superior (CAPES) and the Fundação de Amparo à Pesquisa do Estado de São Paulo (FAPESP), process 2023/00912-1, linked to process 2021/11762-5.

References

Agência Nacional de Águas ANA (Brasil), 2019. Plano Nacional de Segurança Hídrica. Brasília, ANA, 2019.112p.

Archie, G. E., 1942. The electrical resistivity log as an aid in determining some reservoir characteristics: Transactions of the American Institute of Mining and Metallurgical Engineers, 146, 54–62.

Binley, A., Hubbard, S. S., Huisman, J. A., Revil, A., Robinson, D. A., Singha, K., and Slater, L. D., 2015. The emergence of hydrogeophysics for improved understanding of subsurface processes over multiple scales, Water Resour. Res., 51, 3837– 3866, doi:10.1002/2015WR017016.

Blanchy, G., Saneiyan, S., Boyd, J, McLachlan, P., Binley, A., 2020. ResIPy, an intuitive open source software for complex geoelectrical inversion/modeling. Computers & Geosciences, Volume 137, 104423, https://doi.org/10.1016/j.cageo.2020.104423.

Blondel, A., Schmutz, M., Franceschi, M., Tichané, F., and Carles, M., 2014. Temporal Evolution of the geoelectrical response on a hydrocarbon contaminated site. Journal of Applied Geophysics, 103, 161-171, doi: 10.1016/j.jappgeo.2014.01.013.

Brantley, S.L., Goldhaber, M.B., and Ragnarsdottir, V., 2007. Crossing disciplines and scales to understand the Critical Zone. Elements 3, 307-314. doi: 10.2113/gselements.3.5.307.

Brantley, S. L.; Mcdowell, W. H.; Dietrich, W. E.; White, T. S.; Kumar, P.; Anderson, S. P.; Chorover, J.; Lohse, K. A.; Bales, R. C.; Richter, D. D.; Grant, G.; Gaillardet, J., 2017. Designing a network of critical zone observatories to explore the living skin of the terrestrial Earth. Earth Surface Dynamics, v. 5, p. 841–860, 2017, doi: 10.5194/esurf-5-841-2017.

Falzone, S., Robinson, J. & Slater, L., 2019. Characterization and Monitoring of Porous Media with Electrical Imaging: A Review. Transp Porous Med 130, 251–276, doi: 10.1007/s11242-018-1203-2.

FAO (Food and Agriculture Organization of the United Nations), 2014. The Water-Energy-Food Nexus: A new approach in support of food security and sustainable agriculture". Technical Report.

Feitosa, F.A.C. (coord.), 2008. Hidrogeologia: conceitos e aplicações. 3. ed. rev. e ampl. Rio de Janeiro: CPRM: LABHID. 812 p. ISBN 9788574990613. https://rigeo.cprm.gov.br/handle/doc/14818.

Kowalski, A. C. G., 2022. Perfilagem do potencial espontâneo de baixo ruído aplicada ao estudo do fluxo em fraturas. Tese de Doutorado, Instituto de Astronomia, Geofísica e Ciências Atmosféricas, Universidade de São Paulo, SP, 168p.

Leroy, P., Revil, A., Kemna, A., Cosenza, P., and Ghorbani, A., 2008, Complex conductivity of water-saturated packs of glass beads: Journal of Colloid and Interface Science, 321, 103–117, doi: 10.1016/j.jcis.2007.12.031.

Leroy, P., and A. Revil, 2009. A mechanistic model for the spectral induced polarization of clay materials: Journal of Geophysical Research, 114, B10202, doi: 10.1029/2008JB006114.

Martin, T., Titov, K., Tarasov, A., and Weller, A., 2021. Spectral induced polarization: frequency domain versus time domain laboratory data, Geophysical Journal International, Volume 225, Issue 3, June 2021, Pages 1982–2000, https://doi.org/10.1093/gji/ggab071.

Parsekian, A. D., Singha K., Minsley, B. J., Holbrook, W. S., and Slater L., 2015. Multiscale geophysical imaging of the critical zone, Rev. Geophys., 53, 1–26, doi:10.1002/2014RG000465.

Revil, A., 2013. Effective conductivity and permittivity of unsaturated porous materials in the frequency range 1 mHz–1GHz, Water Resour. Res., 49, doi:10.1029/2012WR012700.

Revil, A., and N. Florsch, 2010. Determination of permeability from spectral induced polarization in granular media: Geophysical Journal International, 181, 1480–1498, doi: 10.1111/j.1365-246X.2010.04573.x.

Revil, A., Koch, K., & Holliger, K., 2012. Is it the grain size or the characteristic pore size that controls the induced polarization relaxation time of clean sands and sandstones? Water Resources Research, 48, W05602. https://doi.org/10.1029/2011WR011561.

Robinson, J., Slater, L., Weller, A., Keating, K., Robinson, T., Rose, C., et al., 2018. On permeability prediction from complex conductivity measurements using polarization magnitude and relaxation time. Water Resources Research, 54, 3436–3452. https://doi.org/10.1002/2017WR022034.

Silva, B. P. C., 2019. Hydropedology as support for water resources management in an experimental watershed at mantiqueira mountain range. Tese de Doutorado em Ciência do Solo, Universidade Federal de Lavras, Lavras, 94p.

Slater, L., W. Barrash, J. Montrey, and A. Binley, 2014. Electrical-hydraulic relationships observed for unconsolidated sediments in the presence of a cobble framework, Water Resour. Res., 50, doi:10.1002/2013WR014631.

Ustra, A. T., 2017. Imageamento geofísico para investigações de áreas contaminadas: Imageamento 3D de eletrorresistividade e polarização induzida a jusante de uma área de disposição de resíduos urbanos. Novas Edições Acadêmicas.

Weigand, M., and A. Kemna, 2016. Debye decomposition of time-lapse spectral induced polarisation data: Computers & Geosciences, 86, 34-45, doi: 10.1016/j.cageo.2015.09.021.

Weller, A., Slater, L., Binley, A., Nordsiek, S., and Xu, S., 2015a. Permeability prediction based on induced polarization: Insights from measurements on sandstone and unconsolidated samples spanning a wide permeability range. GEOPHYSICS 2015 80(2), D161-D173. doi: 10.1190/geo2014-0368.1.

Weller, A. and Slater, L., 2019. Permeability estimation from induced polarization: an evaluation of geophysical length scales using an effective hydraulic radius concept. Near Surface Geophysics, 17: 581-594. https://doi.org/10.1002/nsg.12071.